

Axially-symmetric sheared polymer network liquid crystals

Yung-Hsun Wu, Yi-Hsin Lin, Hongwen Ren, Xiangyi Nie, Ju-Hyun Lee,
and Shin-Tson Wu

College of Optics and Photonics, University of Central Florida, Orlando, Florida 32816

swu@mail.ucf.edu

<http://lcd.creol.ucf.edu>

Abstract: An axially-symmetric sheared polymer network liquid crystal (SPNLC) device is demonstrated and its performances characterized. Through analyzing the structure of this axially-symmetric SPNLC, we constructed a 3-D model to explain the observed phenomena. The simulation results agree well with the experiment. Two potential applications of such an axially-symmetric SPNLC, namely tunable-focus negative lens and spatial polarization converter, are discussed.

©2005 Optical Society of America

OCIS codes: (230.3720) Liquid-crystal devices; (160.5470) Polymers

References and links

1. J. H. Lee, H. R. Kim, and S. D. Lee, "Polarization-insensitive wavelength selection in an axially symmetric liquid-crystal Fabry-Perot filter," *Appl. Phys. Lett.* **75**, 859-861 (1999).
2. H. Ren, Y. H. Lin, Y. H. Fan, and S. T. Wu, "Polarization-independent phase modulation using a polymer-dispersed liquid crystal," *Appl. Phys. Lett.* **86**, 141110 (2005).
3. R. Yamaguchi, T. Nose, and S. Sato, "Liquid crystal polarizers with axially symmetrical properties," *Jpn. J. Appl. Phys.* **28**, 1730-1731 (1989).
4. M. Stalder and M. Schadt, "Linearly polarized light with axial symmetry generated by liquid-crystal polarization converters," *Opt. Lett.* **21**, 1948-1950 (1996)
<http://ol.osa.org/abstract.cfm?id=45260>
5. A. Niv, G. Biener, V. Kleiner, and E. Hasman, "Formation of linearly polarized light with axial symmetry by use of space-variant subwavelength gratings," *Opt. Lett.* **28**, 510-512 (2003)
<http://ol.osa.org/abstract.cfm?id=71638>
6. S. C. Tidwell, D. H. Ford, and W. D. Kimura, "Generating radially polarized beams interferometrically," *Appl. Opt.* **29**, 2234-2239 (1990).
<http://ao.osa.org/abstract.cfm?id=37968>
7. Y. H. Wu, Y. H. Lin, Y. Q. Lu, H. Ren, Y. H. Fan, J. R. Wu and S. T. Wu "Submillisecond response variable optical attenuator based on sheared polymer network liquid crystal," *Opt. Express*, **12**, 6377-6384 (2004).
<http://www.opticsexpress.org/abstract.cfm?URI=OPEX-12-25-6382>
8. J. L. West, G. Zhang, and A. Glushchenko, "Fast birefringent mode stressed liquid crystal," *Appl. Phys. Lett.* **86**, 031111 (2005).
9. Y. H. Fan, Y. H. Lin, H. Ren, S. Gauza, and S. T. Wu, "Fast-response and scattering-free polymer network liquid crystals for infrared light modulators," *Appl. Phys. Lett.* **84**, 1233-1235 (2004).
10. A. V. Nesterov and V. G. Niziev, "Laser beams with axially symmetric polarization," *Phys. D: Appl. Phys.* **33**, 1817-1822 (2000).

1. Introduction

An axially-symmetric liquid crystal (LC) structure can be used as a wavelength selection Fabry-Perot filter and a spatial polarization converter. A particularly attractive feature of the axially-symmetric LC structure is that the device is independent of linearly polarized light in the azimuthal angles because the LC directors are oriented symmetrically in the radial

directions. Therefore, we can use it as an optical device which is insensitive to the polarization change [1, 2]. Besides, there is an emerging interest in developing the space-variant polarized light with axial symmetry [3-5]. Several approaches for achieving this kind of spatial polarization characteristic have been explored. One approach uses the interference of two linearly polarized beams [6]. The major shortcoming of this method is the relatively low light efficiency and complicated fabrication process. Others use special LC cells with circular rubbing [3, 4] or subwavelength gratings [5] to realize the radially or azimuthally polarized light. However, these approaches require a complicated fabrication procedure such as circular rubbing or micro-fabrication process.

In this paper, we report a new axially-symmetric sheared polymer network liquid crystal (SPNLC) [7], also known as stressed liquid crystal [8]. In a SPNLC, the response time is decoupled from the LC layer thickness. Through analyzing the structure of this axially-symmetric SPNLC, we constructed a 3-dimensional model to explain the observed phenomena. The simulation results agree well with the experiment. The axially-symmetric SPNLC can be used as a tunable-focus negative lens and a spatial polarization converter.

2. Sample fabrication

To prepare a PNLC cell, we mixed 15 wt % of a photopolymerizable monomer (Norland optical adhesive NOA65) in a commercial Merck E7 LC mixture. The mixed LC and monomer was sandwiched between two ITO (indium-tin-oxide) glass substrates separated by two stripe mylar spacers. The cell gap was controlled at $\sim 9 \mu\text{m}$. To polymerize the LC cell, a two-step UV curing process was adopted [7, 8]. In the first step, the LC cell was illuminated to a UV light ($\lambda \sim 365 \text{ nm}$, $I = 50 \text{ mW/cm}^2$) for 15 min at $T = 110 \text{ }^\circ\text{C}$, which is higher than the clearing temperature of E7 ($\sim 60 \text{ }^\circ\text{C}$). In the second step, the cell was cured in the same condition but at $20 \text{ }^\circ\text{C}$. Since the ITO glass has no surface treatment, the LC domains are randomly distributed so that the cell appears translucent after UV curing. Applying a shearing force along the center of the top substrate while keeping the bottom glass substrate fixed stretches the entangled polymer networks and suppresses the light scattering completely [7, 8]. The sheared PNLC cell is highly transparent at $\lambda > 600 \text{ nm}$. However, if the shearing force is off-axis and the shearing torque is large enough, the polymer networks begin to contract and form an axially-symmetric pattern owing to the restoring force. To control the radial SPNLC patterns, we employed a precise motor motion system (Newport ESP-300) to control the initial acceleration, shearing speed, deceleration, and total shearing distance. The shearing conditions are listed as follows: acceleration = 10 mm/s^2 , speed = 2.5 mm/s , deceleration = -10 mm/s^2 , and shearing distance $\sim 150 \mu\text{m}$. To prevent the sheared LC directors from relaxing back, the peripherals of the cell were sealed by a UV adhesive. All our measurements were performed using the sealed LC cell. No noticeable performance change was detected before and after the sealing.

Figure 1 shows the primitive structure of the axially symmetric SPNLC. After the shearing process, the LC directors align toward the center of the pattern. Polymer network forms a radial structure and constrains the LC directors within a circle. The screen shows the image of the axially symmetric SPNLC structure under the crossed polarizers. The black cross is caused by the passing light whose polarization direction is perpendicular to the transmittance axis of the polarizer or analyzer. In order to verify the axially symmetric properties of the SPNLC structure, we rotated the polarizer/analyzer pairs from 0° to 360° while keeping them crossed. In principle, we could fix the polarizer and analyzer but rotate the sample. The former method is preferred because it keeps the laser beam at the same spot of the sample. Experimental error due to nonuniformity of the sample can thus be ruled out. The experimental results show that the crossed-hair patterns rotate in correspondence of the polarizer/analyzer rotation. The output is identical, independent of the rotation angle of the incident light polarization. This observation confirms that the LC directors indeed are axially symmetric.

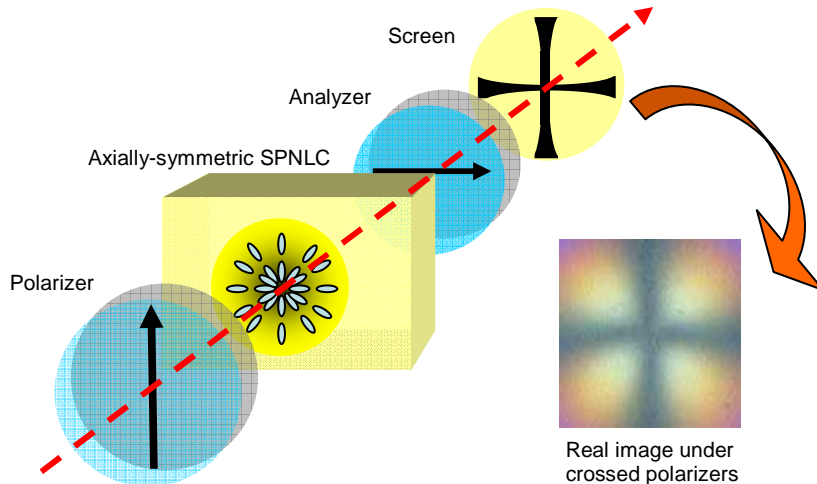


Fig. 1. SPNLC structure observed under crossed polarizers.

3. Experiment and results

Figure 2 shows the polarization independence of the axially-symmetric SPNLC structure to the linearly polarized light in the azimuthal angles. To verify the polarization independence, we measure the voltage-dependent transmittance curves (V-T curve) under three different rotation angles of the crossed polarizers. The input light ($\lambda=632.8$ nm) was expanded and collimated to 10 mm to cover the central portion of the LC sample. The diameter of the whole sample is ~ 20 mm. The reason we narrow down the aperture size to 10 mm is because the central part has better LC alignment and less defects. The V-T curves were measured at three polarizer angles: 0° , 45° , and 90° . The analyzer is always crossed to the polarizer. As shown in Fig. 2, the three V-T curves overlap very well. That means the LC directors are distributed in radial directions, as sketched in Fig. 1.

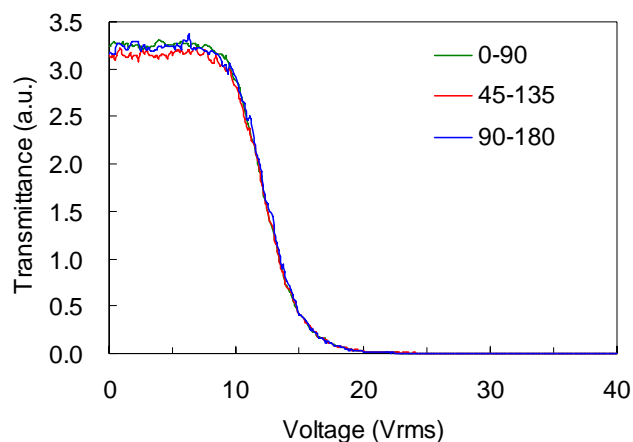


Fig. 2. Voltage-dependent transmittance of the axially symmetric SPNLC cell. $d=9$ μm and $\lambda=633$ nm.

Figures 3(a) and 3(b) show the measured response time of the axially-symmetric SPNLC. To measure the response time, we applied a 20 V_{rms} at $f=1$ kHz square waves to the LC cell. The rise time and decay time are defined from $90\rightarrow 10\%$ and $10\rightarrow 90\%$ transmittance change, respectively. The measured optical response times are recorded in the lower traces. From Figs. 3(a) and 3(b), the measured rise time is 0.6 ms and decay time 1.8 ms. From previous studies

[7, 8], SPNLC exhibit a fast response time because of the small LC domain sizes and, moreover, the response time is insensitive to the cell gap. Thus, we can use a thick cell gap to gain phase change while still keeping a fast response time. The tradeoff of using a thick LC layer is the increased voltage.

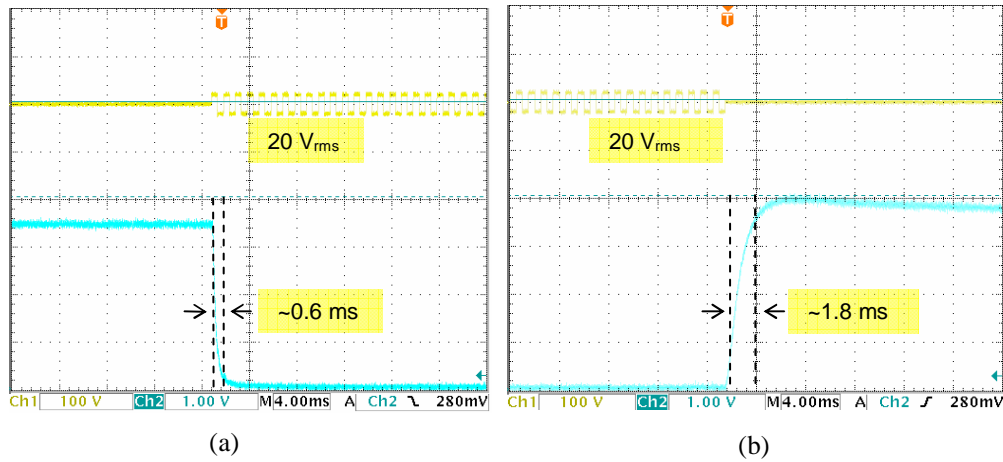


Fig. 3. Optical response time of the 9- μm axially-symmetric SPNLC: (a) rise time, and (b) decay time.

To understand the detailed structure of the axially-symmetric SPNLC, we analyze the phase difference at different positions of the pattern. Figure 4(a) shows the top view and cross-section of the structure. The diameter of the pattern is ~ 20 mm. We measured the phase retardation from the center to the edge of the ring at $V=0$. Figure 4(b) shows the gradient distribution of the phase retardation from the center to the outer ring of the SPNLC structure. The phase difference increases from 0 at center to 450 nm at the edge of the pattern. The different phase retardation in each position at $V=0$ represents the different LC alignment in the initial state. The larger phase retardation implies the lower pretilt angle. Based on the simulation results, the average pretilt angle is larger than 60° .

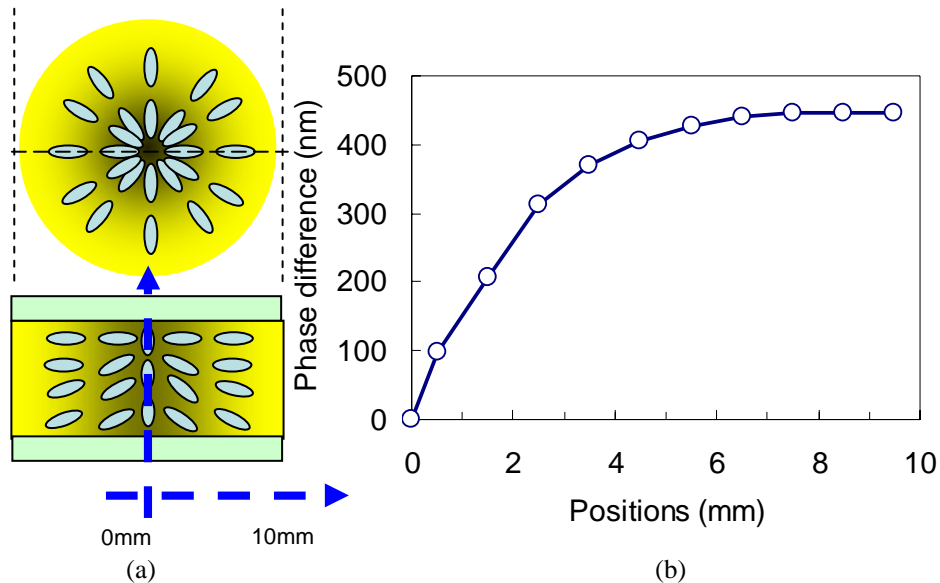


Fig. 4. (a) Top view and cross-section of the LC structure; (b) Measured gradient distribution of the phase retardation.

Figure 5 shows the simulated LC tilt angle distribution. At center, the tilt angle is nearly 90° . That means the LC directors are nearly perpendicular to the substrates. This explains why the central spot always appears dark under crossed polarizers. As the radial distance increases, the tilt angle gradually decreases. At each position of the cross-section, the LC directors possess a hybrid structure, i.e., the LC near the top and bottom substrates have different tilt angles. The relatively large tilt angle helps to lower the threshold voltage and the dark state voltage, but the tradeoff is the reduced phase retardation.

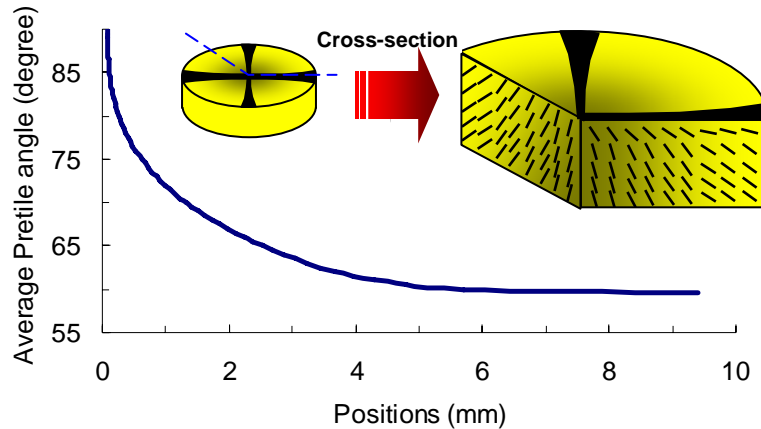


Fig. 5. Simulated pretilt angle distribution of the axially-symmetric SPNLC cell.

Figure 6 plots the measured V-T curves at different radial positions in the pattern. The high driving voltage implies the LC directors are tightly anchored by the polymer networks. It also implies the large elastic constant for the axially-symmetric SPNLC structure. Besides, we should also consider the weak surface boundary condition because there is no surface treatment on the glass substrates. The different transmittance of the V-T curve at the initial point represent the different alignment structure at $V=0$. The higher transmittance means the larger phase retardation. The phase retardation decreases as the position moves toward the center of the pattern.

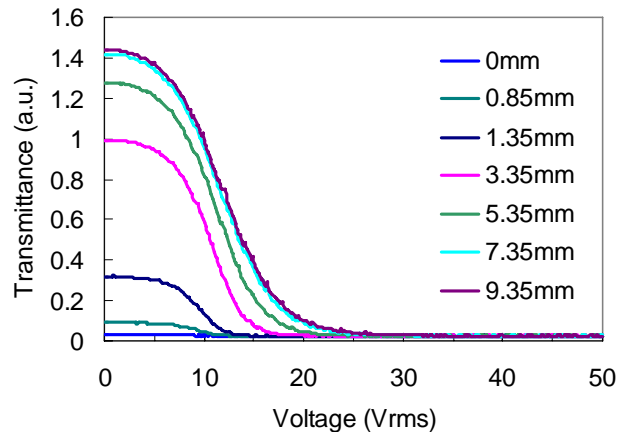


Fig. 6. Measured V-T curves at different positions of the axially-symmetric SPNLC cell.

From Fig. 6, the axially-symmetric SPNLC has a lower threshold voltage than PNLC. This is because the axially-symmetric SPNLC has hybrid LC alignment in each cross-section and the increased tilt angle smears the threshold behavior and lowers the dark state (between crossed polarizers) voltage. On the other hand, a PNLC cell has surface alignment and the employed polymer is quite rigid. The small polymer network domains significantly reduce the response time, but the tradeoffs are the increased threshold and operating voltages [9].

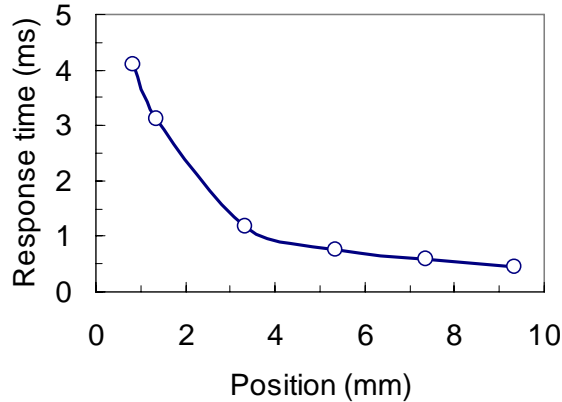


Fig. 7. Measured response time at different positions of the axially-symmetric SPNLC cell.

Figure 7 plots the measured response time at different positions of the axially-symmetric SPNLC. Since the LC tilt angle varies spatially, to reduce experimental error we should keep the laser spot size as small as possible. In our lab, we have a $1.55 \mu\text{m}$ laser whose beam diameter is less than 1 mm. Therefore, we used this laser for the response time measurements. From Fig. 7, the measured response time is slower near the center of the pattern than at the edge. Two reasons contribute to the slower response time observed in the central portion. First, the LC directors near the central section have less restoring force than those in the edge because of the high tilt angles. Second, the central LC directors are bounded by weaker polymer networks which produce a smaller restoring torque than the border.

Figure 8(a) is a movie showing the real dynamic image of the experimental results when a voltage is applied to the axially-symmetric SPNLC. Based on the measured birefringence, V-T curve, and response time at different radial positions of the structure, we construct a 3-dimensional model of the LC directors and simulate the dynamic response under crossed polarizers. Figure 8(b) is a movie showing the simulated results. The simulation results agree quite well with the experiment.

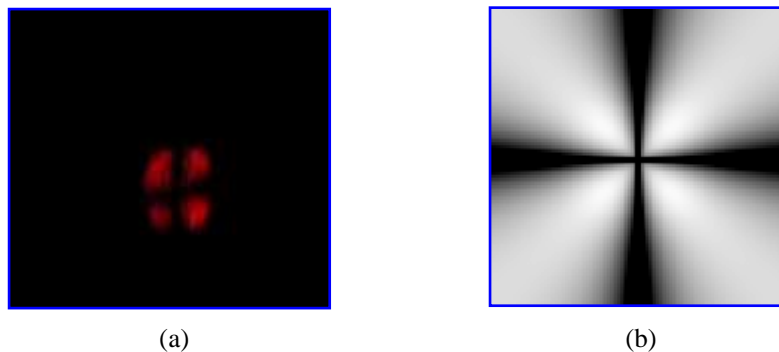


Fig. 8. (a) A movie shows the real dynamic image of the axially-symmetric SPNLC cell (492KB), and (b) Simulation results (443KB).

4. Discussion

The axially-symmetric SPNLC device has potential application as a tunable-focus lens and a spatial polarization converter. For instance, by illuminating with a radially polarized light [10] the axially-symmetric SPNLC cell functions like a tunable-focus lens. At $V=0$, the cell has a natural gradient phase profile from the center to the edge, as shown in Fig. 4(b) so that the lens effect appears. As the voltage increases, the phase profile becomes flatter and the lens effect is gradually vanishing. Since the structure is axially symmetric, the lens performance is independent of the incident light polarization, as shown in Fig. 2.

Another interesting application is the so-called spatial polarization converter. For example, we can make a rotationally symmetric half-wave plate using the axially-symmetric SPNLC cell if its average $d\Delta n$ value is equal to $\lambda/2$ [4]. Figure 9 shows the concept of such a polarization converter for the case of $P=2$; where P is the polarization order number of the polarized light field [4]. In Fig. 9(a), we illuminate a linearly polarized light to this device. The rotationally half-wave plate shown in Fig. 9(b) would rotate the linearly polarized light to a different angle in each position. This is because the $\lambda/2$ wave plate in each position rotates the linearly polarized light to twice the angle which is between the incoming linear polarized light direction and the slow axis. Therefore, the output polarization, as shown in Fig. 9(c) is converted to a circularly symmetric but linearly polarized light field ($P=2$). Thus, the proposed axially-symmetric SPNLC cell will act as a spatial polarization converter.

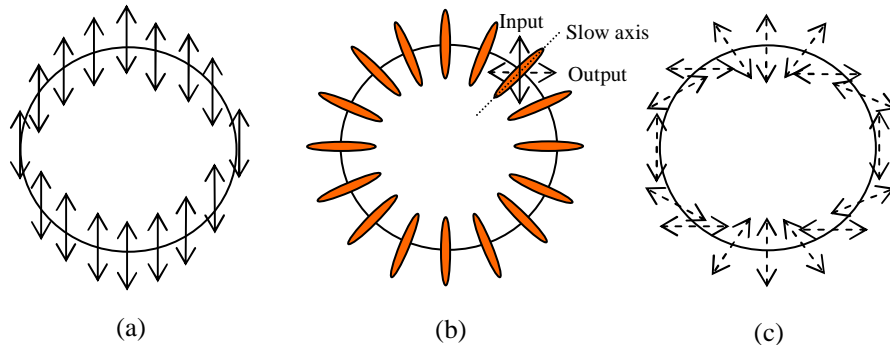


Fig. 9. (a) Incident light with vertical linear polarization, (b) Rotationally symmetric half wave plate, and (c) Output light with polarization $P=2$ field.

5. Conclusion

We have demonstrated an axially-symmetric SPNLC structure for high speed photonics applications. The structure of the axially symmetric SPNLC is analyzed by measuring the birefringence, V - T curve, and response time at different radial positions of the cell. We also construct a 3D model based on the simulation results. The results agree well with our experiment. Its potential applications include a negative tunable-focus LC lens and a spatial polarization converter.

Acknowledgment

This work was supported by AFOSR under Contract No. F49620-01-1-0377. We would like to thank Dr. X. Liang for kindly providing ITO glass substrates.